Supplemental Data

A

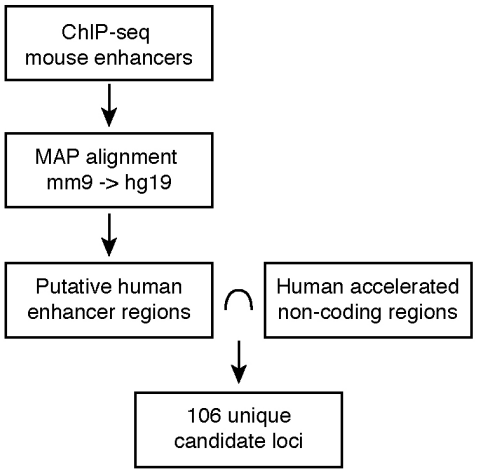

B

Human enhancer	*Hs-HARE1*	*Hs-HARE2*	*Hs-HARE3*	*Hs-HARE4*	*Hs-HARE5*	*Hs-HARE6*
Selection scan	Prabhakar	Bird	Prabhakar, Bird	Prabhakar	Bird	Lindblad-Toh
Chip-seq	H3K4me1	P300	P300	P300	P300	H3K4me1
Forebrain expression / total LacZ+	3/6	2/9	7/18	0/3	15/15	9/12

E14.5

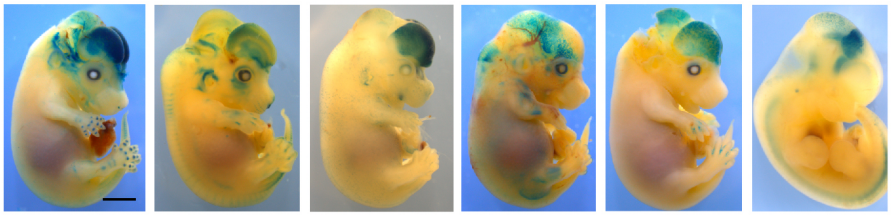

C *Hs-HARE5::LacZ* E14.5

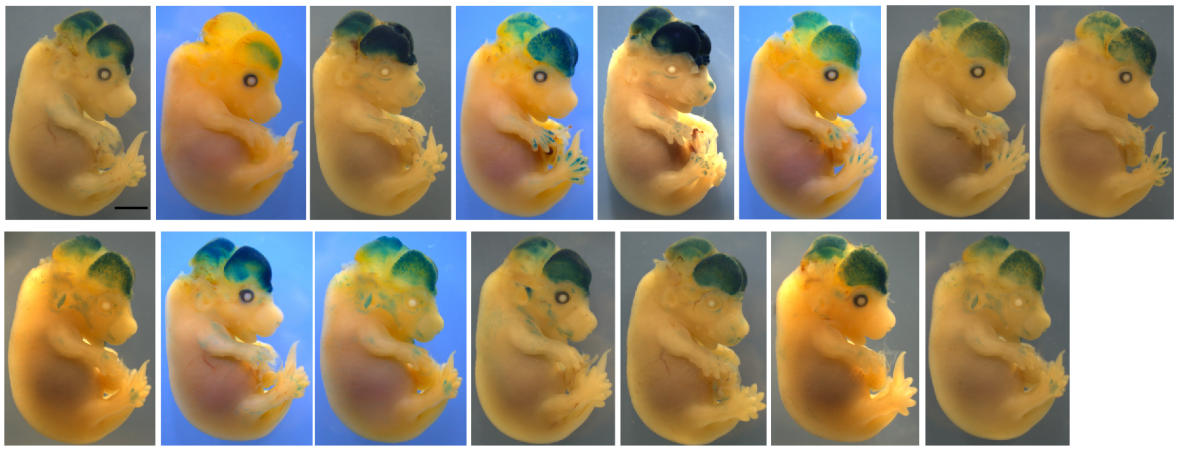

Figure S1, Related to Figure 1. **Screen for evolutionarily important enhancers.** (A) Schematic workflow for identifying human-accelerated brain enhancers, as described in Supplemental Experimental Procedures. 106 unique putative neocortical enhancer loci with signatures of positive selection were identified from the screen (see also Table S1). (B) Images of E14.5 representative transient transgenic embryos for *HARE1-6* assayed for β-galactosidase activity, and listed with relevant information. *HARE1*-6 were prioritized from the screen based on their proximity to genes known or predicted to be involved in corticogenesis. Selection scans are from following references (first author name listed): human-accelerated conserved noncoding sequence [S1]; accelerated conserved noncoding sequence [S2]; and primate accelerated region [S3]. Chip-Seq are from the following references: H3K4me1 [S4], P300 [S5]. *HAREs1, 2,* and *4* showed variable enhancer activity, whereas *HAREs 3, 5*, and *6* demonstrated more consistent LacZ enhancer activity. C) Images of E14.5 transient transgenic embryos for *Hs-HARE*5::*LacZ* assayed for β-galactosidase activity. Note *HARE5* activity in the lateral forebrain and dorso-lateral midbrain, and to a lesser and more variable extent in the spinal cord and retina. Scale bars, 2mm.

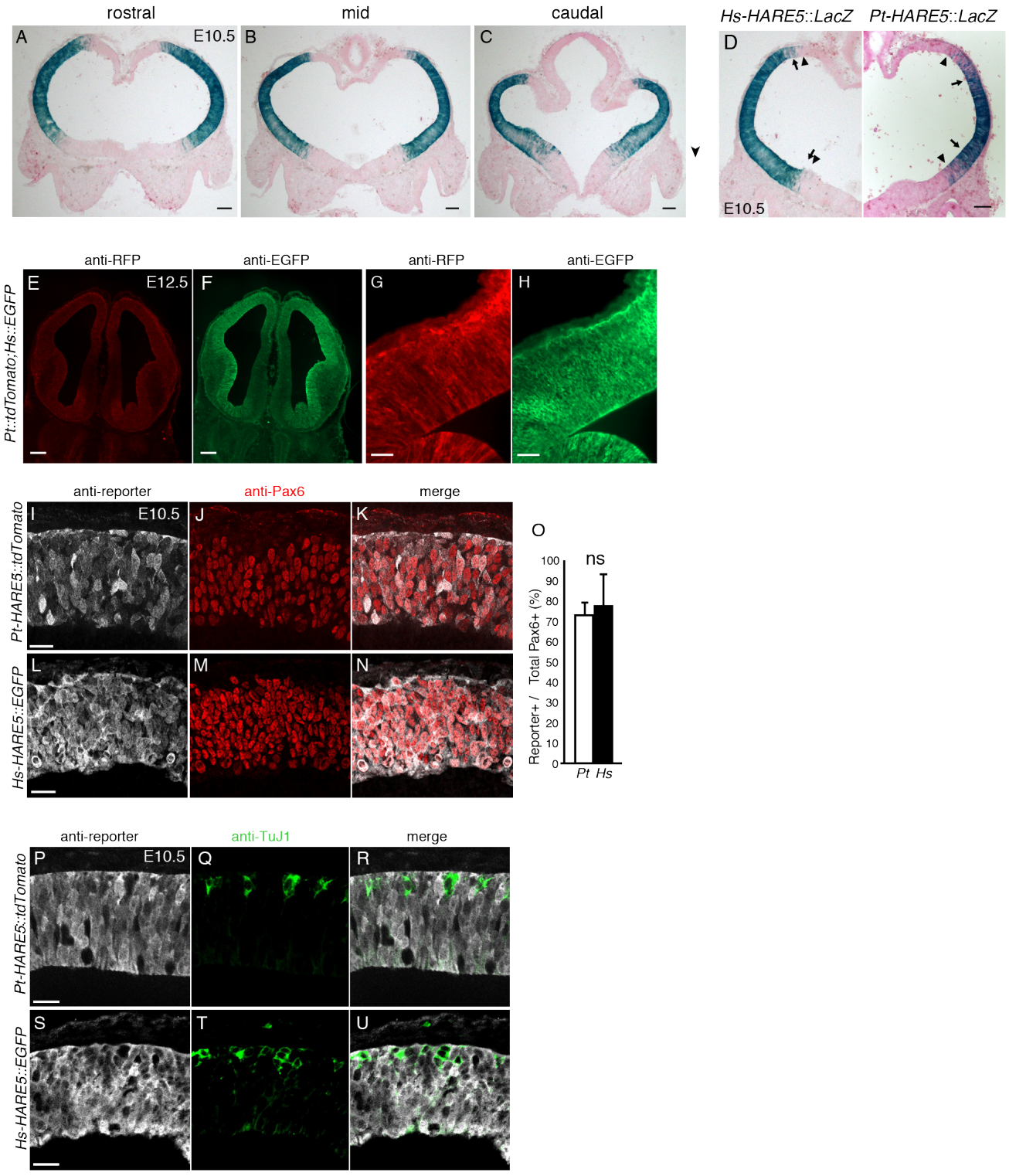
rostral
mid
caudal
A
E10.5
B
C
Hs-HARE5::LacZ
Pt-HARE5::LacZ
D
E10.5
anti-RFP
anti-EGFP
anti-RFP
anti-EGFP
Pt::tdTomato;Hs::EGFP
E
E12.5
F
G
H
anti-reporter
anti-Pax6
merge
Pt-HARE5::tdTomato
I
E10.5
J
K
Hs-HARE5::EGFP
L
M
N
O
ns
Reporter+ / Total Pax6+ (%)
100
90
80
70
60
50
40
30
20
10
0
Pt
Hs
anti-reporter
anti-TuJ1
merge
Pt-HARE5::tdTomato
P
E10.5
Q
R
Hs-HARE5::EGFP
S
T
U

Figure S2, Related to Figure 2. ***HARE5* activity in the lateral telencephalon.** (A-C) Rostral to caudal coronal sections from E10.5 *Hs-HARE5*::*LacZ* brains depicting LacZ activity in the lateral telencephalon with a graded dorso-ventral boundary. (D) Comparison of rostro-caudal matched coronal sections from *Hs-HARE5*::*LacZ* and *Pt-HARE5*::*LacZ* E10.5 embryos. Arrows indicate boundary of uniform LacZ activity and arrowheads indicate boundary of graded LacZ activity. (E-H) Immunofluorescence of E12.5 coronal sections co-expressing *Pt-HARE5*::*tdTomato* and *Hs-HARE5*::*EGFP* at low magnification (E,F) and high-magnification along the lateral wall (G,H), and stained with anti-RFP (E, G) and anti-EGFP (F,H). Note both reporters are active in the VZ/SVZ of the lateral telencephalon. (I-U) Immunofluorescence of E10.5 coronal sections co-expressing *Pt-HARE5::tdTomato* (I-K; P-R) and *Hs-HARE5::EGFP* (L-N; S-U) and stained with anti-RFP (I,P), anti-EGFP (L,S), anti-Pax6 (J,K,M,N) or anti-TuJ1 (Q,R,T,U). Note, *Hs-HARE5* and *Pt-HARE5* activity are high in Pax6-positive neuroepithelial cells but are also evident in some TuJ1-positive neurons. (O) Graph depicting fraction of all Pax6-positive cells that co-stain for either RFP (*Pt*) or EGFP (*Hs*). Note td-Tomato was recognized by anti-RFP. Error bars, s.d. ns, not significant. Scale bars, 100 μm (A-F), 20 μm (G,H), 25 μm (I-N, P-U).

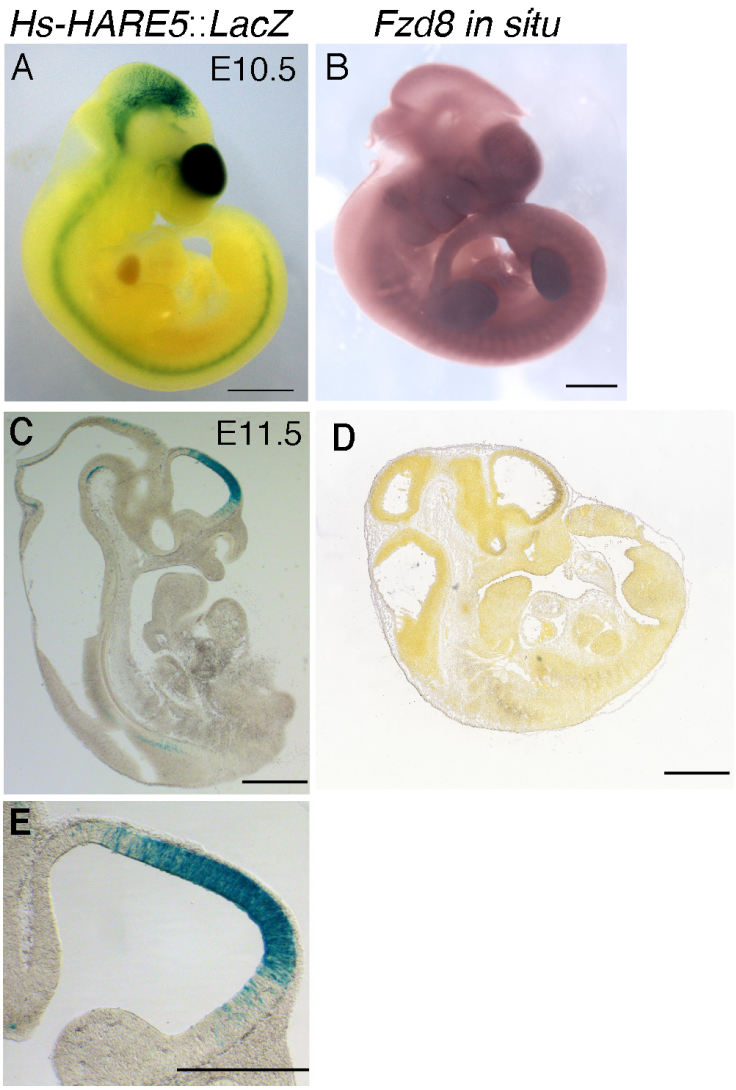

Figure S3, Related to Figure 3. Hs-*HARE5* activity and mouse *Fzd8* mRNA expression. (A-E) E10.5 whole mount lateral views (A,B) and E11.5 sagittal sections (C-E) from *Hs-HARE5*::*LacZ* embryo stained for LacZ activity (A,C,E) or for *in situ* hybridization of mouse *Fzd8* mRNA (B,D). *In situ* images are from www.emouseatlas.org [S6] (B), and http://developingmouse.brain-map.org (D). Note *Hs-HARE5* and *Mm-HARE5* share 51.1% sequence identity, as typical for highly conserved noncoding loci [S2, S3]. (E) High magnification image of *Hs-HARE5*::*LacZ* stained section in C. Scale bars, 1 mm (A-D) 590 μm (E).

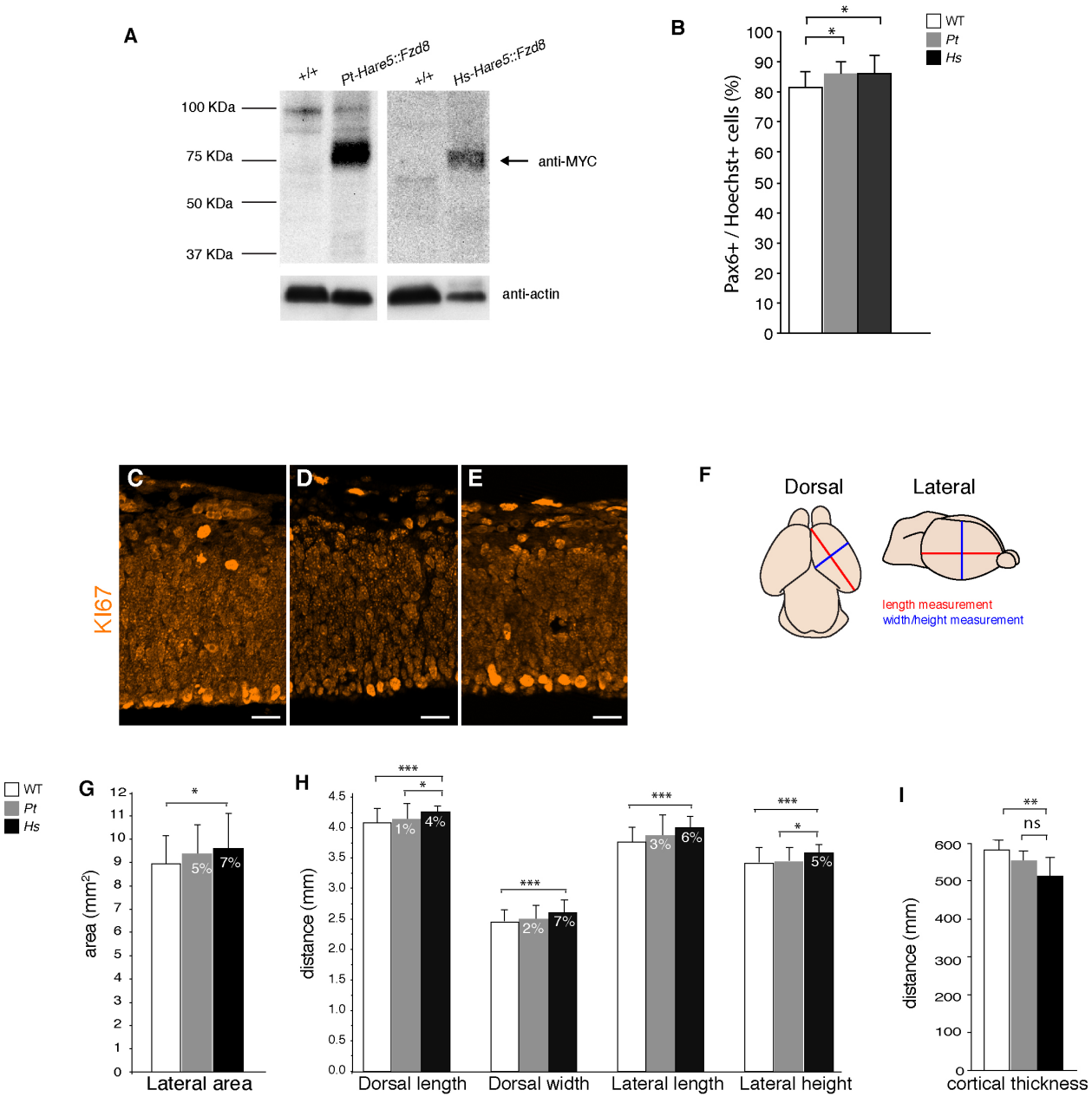

Figure S4, Related to Figure 4. Analysis of *Pt-HARE5::Fzd8* and *Hs-HARE5::Fzd8* brains. (A) Representative western blot of cortices from *Pt-HARE5::Fzd8* and its control littermate (E11.5) and *Hs-HARE5::Fzd8* and its control littermate (E12.5). A 10% SDS-PAGE gel was probed for anti-MYC and anti-Actin, for a loading control. Note a major band of 75KDa evident in both transgenic samples but not in control samples. No

significant difference in MYC levels was detected amongst various samples in replicate westerns. (B) Graph depicting quantification of Pax6-positive cells in control (white box), *Pt-HARE5*::*Fzd8* (gray box), and *Hs-HARE5*::*Fzd8* (black box) brains. (C-E) Coronal E12.5 sections stained for Ki67. (F) Cartoon representation of E18.5 brains with indicated measurements for G,H shown. (G,H) Graphs depicting measurements of E18.5 whole mount brains of indicated genotypes. Note *Hs-HARE5*::*Fzd8* cortices trended to be larger across all measurements, with significance indicated. Included in the bars are the fold increases above WT levels. (I) Graph depicting measurement of coronal sections from E18.5 neocortices of indicated genotypes. Scale bars, C-E, 25 μm. Error bars, s.d., *, $P < 0.05$, **, $P < 0.01$, *** $P<0.001$, ns, not significant.

Epigenetic datasets	Epigenetic mark	P300	Pax6	Sox2	H3K4me1	H3K27ac
	Tissue	E11.5 forebrain [S5]	E12.5 cortex [S9]	E12.5 Neural stem cells [S10]	Neural progenitors [S11]	Neural progenitors [S4]
	# Loci (hg19)	2949	2433	8301	47,258	8,735
Human-accelerated datasets	Prabhakar [S1]	10	0	2	24	4
	Bird [S2]	19	1	2	22	3
	Pollard [S12]	1	0	0	1	0
	Lindblad-Toh (human-accelerated) [S3]	6	0	3	10	0
	Lindblad-Toh (primate-accelerated) [S3]	3	0	4	6	4
Summary	Total intersections (some overlap)	39	1	11	63	11

Table S1. Identification of human/primate-accelerated loci with enhancer marks from *in silico* screen. Related to Figure 1.

Table S2. Transcription factor prediction analysis. Related to Figure 2.

Hs-HARE5 gained binding sites for myc (#1,8,15), a positive regulator of neural stem cell proliferation [S7], and lost binding sites for myc repressors (#8,15), including 2 human-derived and 1 chimpanzee-derived mutations. *Hs-HARE5* lost binding sites for Lef/Tcf (#1,9), which mediates repressor activity in the absence of Wnt signaling, both in human-derived mutations [S8].

Genotype	**Tc (hr)**	**Ts (hr)**	**Tc-Ts (hr)**
WT	12.01 $\pm$ 0.73	6.23 $\pm$ 0.29	5.78 $\pm$ 0.83
Pt	12.15 $\pm$ 1.14	6.34 $\pm$ 0.96	5.81 $\pm$ 0.65
Hs	9.15 $\pm$ 0.88	4.61 $\pm$ 0.41	4.45 $\pm$ 0.65
P-value Hs vs WT	1.5×10^{-4}	2×10^{-5}	0.016
P-value Hs vs Pt	1.4×10^{-4}	0.001	0.003

Table S3. Analysis of cell-cycle kinetics in WT and transgenic E12.5 embryos.

Related to Figure 4.

Supplemental Experimental Procedures

Bioinformatics and *in silico* screen

We propose the term human-accelerated regulatory element (*HARE*) to denote loci that have been bioinformatically identified as rapidly evolving in humans and empirically

demonstrated as *in vivo* enhancers. We identified putative *HAREs* from an *in silico* screen using the following approach (outlined in Figure S1A). Enhancer candidate loci were obtained from publicly available datasets containing empirically identified enhancers. These were derived from ChIP-seq studies of mouse embryonic neocortical tissue or neural stem cells including: p300 [S5], PAX6 [S9], SOX2 [S10], H3K4me1 [S11] and H3K27ac [S4]. We then identified regions of overlap between these enhancer loci and human-accelerated noncoding regions derived from published datasets [S1-3, S12]. All human genomic intervals were then converted to hg19 with the Convert Genome Coordinates tool (v1.0.3) using default settings. Mouse genomic intervals (mm9) were converted to orthologous human coordinates (hg19) with the Extract Pairwise MAF blocks tool (1.0.1) using default settings. MAF blocks were then converted to the BED format using the Maf to BED tool (v.1.0.0) under default parameters. Intersections between human enhancer regions mapped from the mouse genome and human non-coding accelerated regions were determined using the Intersect tool (v.1.0.0) with at least a 1 bp of overlap. Phylogenetic analysis of the *HARE5* locus was performed with MEGA (v5.2.1)[13] on orthologous *HARE5* loci obtained from the UCSC Genome Browser Convert to New Genome tool. We constructed a maximum likelihood tree using the Hasegawa-Kishino-Yano model and a gamma distribution of rates among sites with 5 discrete categories. We utilized the Galaxy Project platform for analyzing genomic datasets [S14].

Sub-cloning of transgenic constructs

For all reporter constructs, enhancer loci were amplified from human genomic DNA (GM12154) and chimpanzee (#5006007) genomic DNA using Phusion High Fidelity Polymerase and directionally cloned into the Gateway entry vector pENTR/D-TOPO (Invitrogen) following the manufacturer's recommendations. DNA reporter constructs were generated containing the original human-accelerated locus, and flanking 5' and 3' sequences, which have been shown to have accessory regulatory motifs required for enhancer activity [S15-17]. Clones were then subcloned into the minimal promoter *hsp68*::LacZ destination vector (kind gift of Len Pennacchio, Lawrence Berkeley National Laboratory). We generated new fluorescent reporter constructs by modifying the minimal promoter *hsp68*::3nls-*CFP-PEST* vector (generous gift from Jèròme Collignon, Universitè Paris-Diderot). The 3xNLS (nuclear localization sequence) was removed by first amplifying the *CFP* gene without the 3xNLS using primers engineered with BamHI (including a Kozak sequence and the first 5 codons of *CFP*) and a BlpI restriction site positioned upstream and downstream, respectively, of the reporter gene. The plasmid was then digested with BamHI and BlpI restriction enzymes, which removed both the 3xNLS and *CFP* reporter, and re-ligated back together with the PCR amplified *CFP* gene lacking the 3xNLS. We subsequently replaced the *CFP* reporter gene with PCR amplified *tdTomato* and *EGFP* genes engineered with BamHI and BlpI restriction sites. Enhancer loci were subcloned into the multiple cloning site of either *hsp68*::*EGFP-PEST* or *hsp68*::*tdTomato-PEST*. Reporter constructs *Hs-HARE5-hsp68*::*EGFP-PEST* (linearized with XbaI, XhoI, and SalI-HF) and *Pt-HARE5-hsp68*::*tdTomato-PEST* (linearized with XhoI, DraIII, and BstB1) were purified by gel

electrophoresis. We generated *Hs-HARE5::Fzd8* and *Pt-HARE5::Fzd8* constructs by first synthesizing mouse *Fzd8* cDNA downstream of the proximal promoter region of hsp68 flanked by XhoI and XbaI restriction sites (GenScript). This cassette was transferred to pCAG using XhoI/XbaI and *Hs/Pt-HARE5* was subcloned with XhoI and EcoNI. All DNA sequences used for transgenic generation were fully sequenced.

Identification of putative transcription factor (TF) binding sites in *HARE5*

To identify potential TF binding sites, we used *in vitro* DNA binding specificity data generated using universal protein-binding microarray (PBM) assays [S18]. PBM data can be used to derive TF-DNA binding motifs, but in addition it yields measurements of TF binding specificity for all possible 8-bp sequences (8-mers), thus providing a more comprehensive view of TF binding preferences compared to DNA motifs. The relative binding preference of a TF for each 8-mer on universal PBMs is quantified by the PBM enrichment score (E-score) [S18, S19] . The E-score is a modified form of the Wilcoxon-Mann Whitney statistic and ranges from -0.5 (least favored sequence) to +0.5 (most favored sequence), with values above 0.35 corresponding, in general, to sequence-specific DNA binding of the tested TF [S18]. We used 612 uPBM data sets for human and mouse TFs from the UniPROBE database and other resources [S20-23]. For each PBM data set, we scanned both the human and the chimpanzee enhancers to identify putative TF binding sites, defined as sites containing at least two consecutive 8-mers with E-score > 0.35, similarly to the procedure used in [S24]. Next, we focused on the specific mutations in the *HARE5* locus, and we identified TFs for which: 1) a putative binding site was predicted in only one of the two lineages, and 2) the difference in E-

score between the human and the chimpanzee site was at least 0.2. The selected TFs were used in the analyses presented in the Table S3.

Mouse genetics and embryonic analysis

All experiments were performed in agreement with the relevant regulatory standards from the Division of Laboratory Animal Resources and IACUC at Duke University School of Medicine. DNA for pronuclear injection was prepared by digesting fully constructs with XhoI/XbaI/SalI-HF (NEB) and purified by electrophoresis (QiaEX II, Qiagen). All linearized constructs were submitted to the Duke Transgenic Mouse Facility for pronuclear injection into 6SJLF1/J strain blastocysts. For the initial screen transient transgenics were tested for enhancer activity using a standard enhancer assay for β-Galactosidase activity. This approach can capture spatial and temporal differences in enhancer function (see [S25, S26] for relevant discussion). For all analyses of *HARE5,* following pronuclear injection, 6SJLF1/J founders were backcrossed to B6/J for subsequent analysis and line propagation. The following lines were generated, with number of lines used shown in parentheses: *Pt-HARE5::LacZ* (3), *Hs-HARE5::LacZ* (4), *Pt-HARE5*::*tdTomatoPEST* (3), *Hs-HARE5*::*EGFP-PEST* (3), *Pt-HARE5*::*Fzd8* (3), and *Hs-HARE5*::*Fzd8* (3). All analyses of enhancer LacZ activity, fluorescence activity, and functional analyses were performed blindly with respect to genotype, and by multiple investigators.

Imaging and immunofluorescence staining of transgenics

LacZ enhancer activity was detected as previously described [S15, S27]. Images of whole-mount LacZ or fluorescent embryos were obtained on a Leica M165 FC microscope using the Leica Application Suite software package (v.4.1.0). For sectioning LacZ embryos, previously fixed embryos were washed in 1X PBS, incubated overnight in 30% sucrose and then embedded in OCT. For sectioning all other embryos, mouse embryos were fixed in 4% paraformaldehyde for 2 hrs. at room temperature or overnight at 4^{o}C and washed 3 x 5 min in 1X PBS solution before an overnight incubation with 30% sucrose at 4^{o}C prior to OCT embedding. Tissue sections were cut 20 μm thick on a cryostat and transferred to Super-Frost Plus slides (Thermo Scientific). Tissue sections were permeabilized with 0.25% triton-X100 in PBS, stained in primary antibodies for 2 hr. at room temperature or overnight at 4^{o}C as previously described [S28] using the following antibodies: mouse anti-TuJ1 (Covance, 1:400), rabbit anti-Pax6 (Millipore, 1:1,000), mouse anti-Pax6 (DSHB, 1:64), mouse anti-MYC (Cell Signaling, 1:200), rabbit anti-Ki67 (Abcam, 1:200), rabbit anti-RFP (Rockland, 1:400), rabbit anti-Foxp1 (Abcam, 1:200), rabbit anti-Foxp2 (Abcam, 1:1000), and chicken anti-EGFP (Abcam, 1:200). EdU stained sections were obtained using Click-iT EdU Alexa Fluor 594 Imaging Kit (Invitrogen) using manufacturer specifications. Fluorescent images were collected on a Zeiss Observer Z1 microscope using ApoTome optical sectioning. Images of native fluorescent proteins were acquired using the Zeiss 43 HE DsRed (Excitation: 545/15) and 38 HE Green Fluorescent (Excitation: 470/40) and Leica GFP3 ET (Excitation: 470/40) and DSR ET (Excitation: 545/30) filter sets.

RT-qPCR Analysis

RNA was extracted from microdissected E10.5 mouse neocortices stored in TRI reagent (Sigma, Cat #T9424) and stored at -80˚C. RNA was extracted according to manufacturer recommendations. RNA samples were treated with DNaseI and cDNA was synthesized with iScript cDNA Synthesis Kit (Bio-Rad, Cat # 170-8891). qPCR was performed using FastStart Universal SYBR Green Master (Rox) (Roche Applied Science Cat # 04913922001) or Fast SYBR Green Master Mix (Applied Biosystems, Cat # 4385612) using cycling conditions recommended by the manufacturer on an ABI StepOnePlus Real-Time PCR machine. Primers (see Table S4) for tdTomato and EGFP were designed using Primer3 (v.0.4.0) in order to produce similarly sized amplicons under identical cycling conditions. Similar amplification efficiencies for both primer sets were obtained.

Chromosomal Confirmation Capture (3C) Analysis

3C assays were performed as previously described [S29]. Embryonic neocortices and reference liver tissues were obtained from pools of 10-16 E12.5 embryos. Neocortical dissections included both the dorsal and ventral telencephalon. Tissue samples were dissociated in 0.125% collagenase type I shaking for 1-2 hr. at 37˚C and fixed with 2% formaldehyde/10%FBS/PBS for 10 min at room temperature. Cell nuclei were prepared from aliquots of 10 million cells and stored at -80˚C until chromatin preparation. Cell nuclei were digested with HindIII (New England BioLabs) overnight and re-ligated with T4 DNA ligase-HC (Promega) for 1-2 days. Control template DNA for quantification of

3C ligation products and normalization was generated from HindIII digested and re-ligated BAC DNA covering the mouse *HARE5* (RP23-137B19; CHORI), *mFzd8* (RP23-292B21; CHORI), and *Ercc3* (RP23-148C24; CHORI) internal control locus. Re-ligation events from chromatin and BAC DNA preparations were detected using TaqMan Gene Expression Master Mix (Applied Biosystems) and double-dye labeled oligonucleotide probes (PrimeTime Integrated DNA Technologies). All reactions were performed in quadruplicate. Quantification of ligation events were determined from standard curves of re-ligated BAC DNA covering the locus of interest and normalized against the internal control *Ercc3* locus. Measurements are reported from at least four biological replicates.

Cell cycle analysis and quantitation

Analysis of cell-cycle kinetics was performed as previously described [S30, S31]. Briefly, pregnant dams were injected with BrdU at T=0 (70 μg/g of body weight), EdU (10 μg/g of body weight) at T=1.5 hours, and sacrificed at T=2 hrs. Embryos were immediately fixed in 4% paraformaldehyde overnight, and embedded in OCT, and then cryosectioned. For detection of BrdU, samples were citrate boiled (Vector Laboratories, Cat H-3300) for at least 30 min at 98^{o}C and then incubated 2 hrs with rat anti-BrdU (1:200, Abcam) followed by addition of secondary anti-rat (1:400, Molecular Probes). Detection of EdU was performed after secondary antibody incubation under conditions specified by the manufacturer (Life Technologies, Click-iT 594 or 647). Calculation of total cell cycle length (Tc) and length of S phase (Ts) were performed as follows: the portion of cells actively in the S-phase cells (S cells) was determined from the number of

EdU+ cells, the leaving fraction (L cells) was determined by the number of BrdU+/EdU- cells, the total number of proliferating cells (P cells) was determined by Ki67+ cells (1:100). Quantification of all cell cycle parameters were determined with at least 5 nonconsecutive slides stained for each marker and were counted blind to genotype using ImageJ software. Quantification of Foxp1 and Foxp2 neurons and Pax6 progenitors was performed using radial columns of coronal cortical sections counted with Image J software. For E18.5 brains, images of E18.5 embryos were captured using a Leica M165 FC microscope with the Leica Application Suite software package (v.4.1.0). Quantitation of tangential length (the distance between posterior and anterior boundaries of the ventricle in sagittal sections), cortical thickness (measured in coronal sections), and whole mount cortical measurements were performed using ImageJ (v1.48s). Measurements were made blind to genotype.

Western blotting

Cortical protein samples and Western blotting were performed as previously shown, with the following exception, per suggestion of Dr. Hiro Matsunami [S28]. In order to resolve and have optimal transfer of the membrane protein, gels were transferred overnight in cold at 16 volts, and samples in SDS-Page buffer were not boiled but instead warmed at room temperature for 2 hours. Blots were probed with mouse anti-Myc (Cell Signaling, 1:1000) and mouse anti-actin (Sigma, 1:200).

HARE Primers	
HARE1.F	CACCCCACTCACTCCACAAGCATC
HARE1.R	GAATTGCCACTTCTCTCCACA
HARE2.F	CACCTCTCCCCAGTTGGATAGAGTAA
HARE2.R	ACCACACTTGAGGCTCTGGA
HARE3.F	CACCTGACCAAGACAGAAGGGAAAA
HARE3.R	ATTTGCTTGGAAAAAGAACCA
HARE4.F	CACCGACATGCACTCTCCTCTCCTG
HARE4.R	AGGGAGACTGATTTTCAAGCA
HARE5 .F	CACCCACAGAGGTTGGGGCACA
HARE5.R	CCAGTGGAAGGCGATAAGAG
HARE6.F	CACCGGGAGAAGGAAAAACGAAGG
HARE6.R	TATTGCTTGAATTGCCCAAAC
Sub cloning Primers	
CFP.BamHI	ATTAGGATCCGCCACCATGGTGAGCAAGGG
CFP.BlpI	AGCCATGGCTAAGCTTCTTGTACAGCTC
td.tomato.BamHI	ATTAGGATCCAGCCACCATGGTGAGCAAGGG
td.tomato.BlpI	GCATGATGCTAAGCTTGACGGTCCGCTTGTACA
EGFP.BamHI	ATTAGGATCCAGCCACCATGGTGAGCAAGGGC
EGFP.BlpI	CCATGGCTAAGCAATCTAGATCCGGTGGA
RT-qPCR Primers	
tdTomato.F	ACCATCGTGGAACAGTACGAG

tdTomato.R	CTTGAAGCGCATGAACTCTTT
EGFP.F	GAAGCAGCACGACTTCTTCAA
EGFP.R	AAGTCGATGCCCTTCAGCTC
GAPDH.R	ACCACAGTCCATGCCATCAC
GAPDH.R	CACCACCCTGTTGCTGTAGCC
3C Primers	
Ercc3.F	GCCCTCCCTGAAAATAAGGA
Ercc3.R	GACTTCTCACCTGGGCCTACA
Mm-HARE5 constant	AGTCTGAGCACCAAATTCAGG
Mm-Fzd8.Test1	TCCTTTCAGACACAAGCATAAG
Mm-Fzd8.Test2	GATGGATTTCCAGAGTGGTTG
Mm-Fzd8.Test3	TTGGCCTTTGTTCTACTTGAG
Mm-Fzd8.Test4	CAAAGAGAAGTTTGAACAAGCA
Mm-Fzd8.Test5	GGCACAGAAAAATGGAGAAAT
Mm-Fzd8.Test6	TTGACAGTGTCCTTTGCCTTA
3C TaqMan Probes	
Mm-HARE5	AAATGAATTATTTTCCAAGTTGAATCA-BQH
Ercc3	AAAGCTTGCACCCTGCTTTAGTGGCC-BQH

Table S4. List of primers used. Related to Experimental procedures.

Supplemental References

S1. Prabhakar, S., Noonan, J. P., Pääbo, S., and Rubin, E. M. (2006). Accelerated evolution of conserved noncoding sequences in humans. Science *314*, 786.

S2. Bird, C. P., Stranger, B. E., Liu, M., Thomas, D. J., Ingle, C. E., Beazley, C., Miller, W., Hurles, M. E., and Dermitzakis, E. T. (2007). Fast-evolving noncoding sequences in the human genome. Genome Biol *8*, R118.

S3. Lindblad-Toh, K., Garber, M., Zuk, O., Lin, M. F., Parker, B. J., Washietl, S., Kheradpour, P., Ernst, J., Jordan, G., Mauceli, E., et al. (2011). A high-resolution map of human evolutionary constraint using 29 mammals. Nature *478*, 476–482.

S4. Creyghton, M. P., Cheng, A. W., Welstead, G. G., Kooistra, T., Carey, B. W., Steine, E. J., Hanna, J., Lodato, M. A., Frampton, G. M., Sharp, P. A., et al. (2010). Histone H3K27ac separates active from poised enhancers and predicts developmental state. Proceedings of the National Academy of Sciences *107*, 21931–21936.

S5. Visel, A., Blow, M. J., Li, Z., Zhang, T., Akiyama, J. A., Holt, A., Plajzer-Frick, I., Shoukry, M., Wright, C., Chen, F., et al. (2009). ChIP-seq accurately predicts tissue-specific activity of enhancers. Nature *457*, 854–858.

S6. Summerhurst, K., Stark, M., Sharpe, J., Davidson, D., and Murphy, P. (2008). 3D representation of Wnt and Frizzled gene expression patterns in the mouse embryo at embryonic day 11.5 (Ts19). Gene Expression Patterns *8*, 331–348.

S7. Kerosuo, L., Piltti, K., Fox, H., Angers-Loustau, A., Hayry, V., Eilers, M., Sariola, H., and Wartiovaara, K. (2008). Myc increases self-renewal in neural progenitor cells through Miz-1. J Cell Sci *121*, 3941–3950.

S8. Freese, J. L., Pino, D., and Pleasure, S. J. (2010). Wnt signaling in development and disease. Neurobiology of Disease *38*, 148–153.

S9. Sansom, S. N., Griffiths, D. S., Faedo, A., Kleinjan, D.-J., Ruan, Y., Smith, J., van Heyningen, V., Rubenstein, J. L. R., and Livesey, F. J. (2009). The level of the transcription factor Pax6 is essential for controlling the balance between neural stem cell self-renewal and neurogenesis. PLoS Genet *5*, e1000511.

S10. Engelen, E., Akinci, U., Bryne, J. C., Hou, J., Gontan, C., Moen, M., Szumska, D., Kockx, C., van IJcken, W., and Dekkers, D. H. (2011). Sox2 cooperates with Chd7 to regulate genes that are mutated in human syndromes. Nature Publishing Group *43*, 607–611.

S11. Meissner, A., Mikkelsen, T. S., Gu, H., Wernig, M., Hanna, J., Sivachenko, A., Zhang, X., Bernstein, B. E., Nusbaum, C., Jaffe, D. B., et al. (2008). Genome-scale DNA methylation maps of pluripotent and differentiated cells. Nature *454*, 766–770.

S12. Pollard, K. S., Salama, S. R., King, B., Kern, A. D., Dreszer, T., Katzman, S., Siepel, A., Pedersen, J. S., Bejerano, G., Baertsch, R., et al. (2006). Forces shaping the fastest evolving regions in the human genome. PLoS Genet *2*, e168.

S13. Tamura, K., Peterson, D., Peterson, N., Stecher, G., Nei, M., and Kumar, S. (2011). MEGA5: molecular evolutionary genetics analysis using maximum likelihood, evolutionary distance, and maximum parsimony methods. Mol. Biol. Evol. *28*, 2731–2739.

S14. Goecks, J., Nekrutenko, A., Taylor, J., Galaxy Team (2010). Galaxy: a comprehensive approach for supporting accessible, reproducible, and transparent computational research in the life sciences. Genome Biol *11*, R86.

S15. Prabhakar, S., Visel, A., Akiyama, J. A., Shoukry, M., Lewis, K. D., Holt, A., Plajzer-Frick, I., Morrison, H., FitzPatrick, D. R., Afzal, V., et al. (2008). Human-Specific Gain of Function in a Developmental Enhancer. Science *321*, 1346–1350.

S16. Bae, B.-I., Tietjen, I., Atabay, K. D., Evrony, G. D., Johnson, M. B., Asare, E., Wang, P. P., Murayama, A. Y., Im, K., Lisgo, S. N., et al. (2014). Evolutionarily dynamic alternative splicing of GPR56 regulates regional cerebral cortical patterning. Science *343*, 764–768.

S17. Capra, J. A., Erwin, G. D., McKinsey, G., Rubenstein, J. L. R., and Pollard, K. S. (2013). Many human accelerated regions are developmental enhancers. Philosophical Transactions of the Royal Society B: Biological Sciences *368*, 20130025.

S18. Berger, M. F., Philippakis, A. A., Qureshi, A. M., He, F. S., Estep, P. W., and Bulyk, M. L. (2006). Compact, universal DNA microarrays to comprehensively

determine transcription-factor binding site specificities. Nat. Biotechnol. *24*, 1429–1435.

S19. Berger, M. F., and Bulyk, M. L. (2006). Protein binding microarrays (PBMs) for rapid, high-throughput characterization of the sequence specificities of DNA binding proteins. Methods Mol Biol *338*, 245–260.

S20. Robasky, K., and Bulyk, M. L. (2011). UniPROBE, update 2011: expanded content and search tools in the online database of protein-binding microarray data on protein-DNA interactions. Nucleic Acids Res *39*, D124–8.

S21. Weirauch, M. T., Cote, A., Norel, R., Annala, M., Zhao, Y., Riley, T. R., Saez-Rodriguez, J., Cokelaer, T., Vedenko, A., Talukder, S., et al. (2013). Evaluation of methods for modeling transcription factor sequence specificity. Nat. Biotechnol. *31*, 126–134.

S22. Gordân, A. M. A. R. (2013). Distinguishing between Genomic Regions Bound by Paralogous Transcription Factors. 1–13.

S23. Gifford, C. A., Ziller, M. J., Gu, H., Trapnell, C., Donaghey, J., Tsankov, A., Shalek, A. K., Kelley, D. R., Shishkin, A. A., Issner, R., et al. (2013). Transcriptional and epigenetic dynamics during specification of human embryonic stem cells. Cell *153*, 1149–1163.

S24. Gordân, R., Shen, N., Dror, I., Zhou, T., Horton, J., Rohs, R., and Bulyk, M. L. (2013). Genomic regions flanking E-box binding sites influence DNA binding

specificity of bHLH transcription factors through DNA shape. CellReports *3*, 1093–1104.

S25. Hubisz, M. J., and Pollard, K. S. (2014). Exploring the genesis and functions of Human Accelerated Regions sheds light on their role in human evolution. Curr Opin Genet Dev *29C*, 15–21.

S26. Enard, W. (2014). Mouse models of human evolution. Curr Opin Genet Dev *29C*, 75–80.

S27. Silver, D. L., Hou, L., Somerville, R., Young, M. E., Apte, S. S., and Pavan, W. J. (2008). The secreted metalloprotease ADAMTS20 is required for melanoblast survival. PLoS Genet *4*, e1000003.

S28. Silver, D. L., Watkins-Chow, D. E., Schreck, K. C., Pierfelice, T. J., Larson, D. M., Burnetti, A. J., Liaw, H.-J., Myung, K., Walsh, C. A., Gaiano, N., et al. (2010). The exon junction complex component Magoh controls brain size by regulating neural stem cell division. Nat Neurosci *13*, 551–558.

S29. Hagège, H., Klous, P., Braem, C., Splinter, E., Dekker, J., Cathala, G., de Laat, W., and Forné, T. (2007). Quantitative analysis of chromosome conformation capture assays (3C-qPCR). Nat Protoc *2*, 1722–1733.

S30. Quinn, J. C., Molinek, M., Martynoga, B. S., Zaki, P. A., Faedo, A., Bulfone, A., Hevner, R. F., West, J. D., and Price, D. J. (2007). Pax6 controls cerebral cortical cell number by regulating exit from the cell cycle and specifies cortical cell identity

by a cell autonomous mechanism. Dev Biol *302*, 50–65.

S31. Martynoga, B. S., Morrison, H., Price, D. J., and Mason, J. O. (2005). Foxg1 is required for specification of ventral telencephalon and region-specific regulation of dorsal telencephalic precursor proliferation and apoptosis. Dev Biol *283*, 113–127.